CHINESE OPTICS LETTERS

Vol. 19, No. 11 | November 2021

Multi-distributed probabilistically shaped PAM-4 system for intra-data-center networks

Mengli Liu (刘梦丽), Mingyi Gao (高明义)*, and Junchi Ke (柯俊驰)

Jiangsu Engineering Research Center of Novel Optical Fiber Technology and Communication Network, Suzhou Key Laboratory of Advanced Optical Communication Network Technology, School of Electronic and Information Engineering, Soochow University, Suzhou 215006, China

*Corresponding author: mygao@suda.edu.cn

Received July 29, 2021 | Accepted September 6, 2021 | Posted Online October 9, 2021

Probabilistically shaped (PS) pulse amplitude modulation (PAM) is a promising technique for intra-data-center networks due to its superior performance, for which a low-complexity and cost-effective distributed matching method is critical. In this work, we propose an energy-level-assigned method to yield PS-PAM-4 signals with various bit rates based on variable probabilistic distributions. We experimentally demonstrate the proposed method in a 25 Gbaud PS-PAM-4 transmission over a bandwidth of approximately 10 GHz. Compared to a uniform PAM-4 system, the proposed multi-distributed PS-PAM-4 system approaches the hard decision threshold at a wide range of received optical power for different applications.

Keywords: probabilistic shaping; pulse amplitude modulation; feed-forward equalizer.
DOI: 10.3788/COL202119.110604

1. Introduction

Data-center traffic has experienced exponential growth over the past decade with high-bandwidth internet applications such as cloud computing/storage, artificial intelligence, and high-definition television. For intra-data-center networks with 2 km links, low cost and low complexity are key requirements, where the intensity-modulation direct-detection (IM/DD) four-level pulse amplitude modulation (PAM-4) with simpler structure and lower energy consumption outperforms other schemes[1–3]. To further enhance the performance and flexibility of a PAM system, probabilistic shaping was introduced, which reduces average signal energy by spherically confining modulation levels in the signal space and thus, relaxes signal-to-noise ratio (SNR) requirements[4]. Unilateral Maxwell–Boltzmann (MB) distribution and unilateral pairwise MB distribution have been proposed for IM/DD systems with optical amplification[5,6]. Bilateral inverse MB distribution was demonstrated in IM/DD systems without optical amplification, and the optimal distribution is symmetric around average power constraint[7]. In addition to optimizing the probabilistic distribution, distributed matcher (DM) should be taken into account as well due to its high computational complexity in the conventional probabilistic shaping schemes. The hierarchical DM has a fully parallel input–output interface and pipelined architecture to perform DM/inv-DM efficiently at the expense of significant rate loss and higher required SNR[8]. The m-out-of-n DM utilizes the scaling and rounding technique, which is challenging in hardware implementation[9]. Constant composition distribution matching (CCDM) based on arithmetic coding has the advantage of zero rate loss[10], but its serial coding process may induce cascaded errors in decoding[11]. Although the DM based on Hoffman coding has lower implementation complexity, it suffers from varying bit rate and synchronization issues[12]. Thus, a probabilistic shaping scheme with reduced complexity and high performance is more desirable in cost-sensitive IM/DD systems, for which a cut-and-paste (CAP) method with lower complexity is a promising candidate[13]. However, the CAP method increases the usage of multipliers and comparators because two mappings are implemented to select sequences with lower energy. Moreover, the chosen sequences with lower energy always have low information rate (IR) and determined distribution.

In this work, we propose an energy-level-assigned (ELA) DM to generate multi-distributed probabilistically shaped PAM-4 (PS-PAM-4) signals. Similar to the above CAP method, the transmitted sequence is first divided into many n-symbol groups, and then, after bit-to-symbol mapping, amplitude bits are extracted. To avoid amounts of calculation and comparison on the original amplitude bits' energies in the conventional CAP method, the proposed ELA method introduces the energy levels into the look up table (LUT). Here, the energies of various n-symbol groups are pre-calculated and classified into different levels. Depending on various application scenarios, different energy-level mapping rules are assigned to yield variable probability distribution. We experimentally demonstrate a 25 Gbaud PS-PAM-4 transmission, and four probability distributions are yielded by varying the assignment of energy levels. Meanwhile,

in order to mitigate the inter-symbol interference (ISI) of 50 Gb/s PS-PAM-4 signal in a 10 GHz bandwidth-limited system, we utilize a feed-forward equalizer (FFE) in the back-to-back (BTB) and 2 km standard single-mode fiber (SSMF) transmission experiments and achieve enlarged opening of the eye diagrams.

2. Principle

Figure 1 shows the block diagram of the probabilistic shaping implementation based on the proposed ELA method. Considering the codebook size and the convenience of presentation, we take three-symbol coding as an example.

Since there is one amplitude bit for each PAM-4 symbol, a three-symbol group has three amplitude bits. The uniform bit sequence u is first divided into the sign bits $[b(S_1)\ldots b(S_{\gamma nc})]$ and the amplitude bits $[b(A_1)\ldots b(A_{nc})]$, respectively, as shown by black numbers and blue numbers in Fig. 1. In order to realize the bilateral MB distribution, the amplitude bits of n symbols are grouped and launched into the DM. Here, a redundant label bit is introduced for each three-amplitude bit, as shown by red numbers in Fig. 1. For the label bits, "0" denotes an inversion operation to yield an n-symbol group with a lower energy level, and "1" indicates a no operation status. The inversion rule depends on the energy levels and will be discussed later in detail. By assigning the symbols with lower energy levels to replace the original sequence, the PS signal is generated. Following the operations of amplitude and sign multiplexing, symbol mapping, channel transmitting, and symbol de-mapping, the inverse DM operation is implemented with label bits generated at the transmitter.

In the scheme, the label bits as additional sign bits are transmitted, and, in order to keep the uniform distribution of sign bits, we invert the last half of the label bits before symbol mapping, and then perform the inverse operation at the receiver. We define the DM rate R_{DM} as the ratio of the number of input bits to the number of output bits of the DM. With an additional bit per n symbols, the DM rate can be calculated as

$$R_{\mathrm{DM}} = m'n/(m'n+1), \tag{1}$$

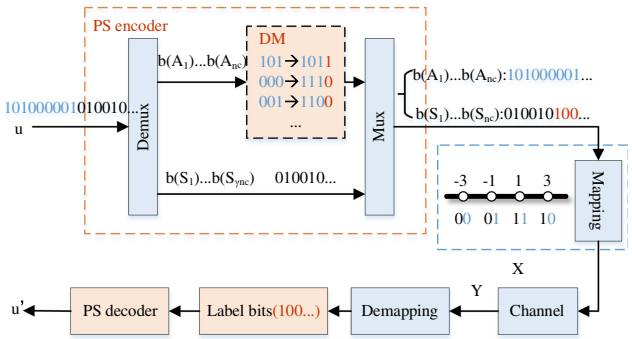

Fig. 1. Block diagram of PS structure based on the proposed ELA method.

Table 1. Energy of Each Combination for Three-Symbol ELA.

Amp bits	000	001	010	011	100	101	110	111
Energy	27	19	19	11	19	11	11	3

where m' is the number of amplitude bits for each PAM symbol. Since every n-sign bit contains one label bit, the fraction γ of sign bits with information is represented by

$$\gamma = (n-1)/n. \tag{2}$$

For a given DM rate R_{DM}, the fraction γ is described as

$$\gamma = 1 + m' - m'/R_{\mathrm{DM}}. \tag{3}$$

Next, the method of energy-level assignment will be presented in detail. We use the Gray code for PAM-4 mapping, where "0" and "1" as sign bits represent "−" and "+", and "0" and "1" as amplitude bits correspond to "3" and "1", respectively. As shown in Fig. 1, the amplitude bits are divided into 3 bit groups before implementing DM. Thus, there are 2^3 permutations and combinations, as shown in the first row of Table 1. The energy of each combination is pre-calculated by

$$E = \sum_{i=1}^{n} x_i^2, \tag{4}$$

where x represents the amplitude value, and n indicates the number of bits in each combination. The energy of each combination is shown in Table 1. For example, "000" denotes a group of three amplitude bits with the amplitude value of "3," and its energy is $3^2+3^2+3^2=27$. Hence, a uniform three-symbol combination will have four energy levels, i.e., E_1, E_2, E_3, and E_4, whose probabilities are 1/8, 3/8, 3/8, and 1/8, respectively, as shown in the first row in Fig. 2, where $E_1 > E_2 > E_3 > E_4$. Consequently, the energy of the transmission sequence can be decreased by reducing the probability of the symbols with a high energy level, which can be implemented simply by inverting bits of high energy levels into that of low energy levels. The detailed inversion rules are shown in Fig. 2. For example, the PS-PAM

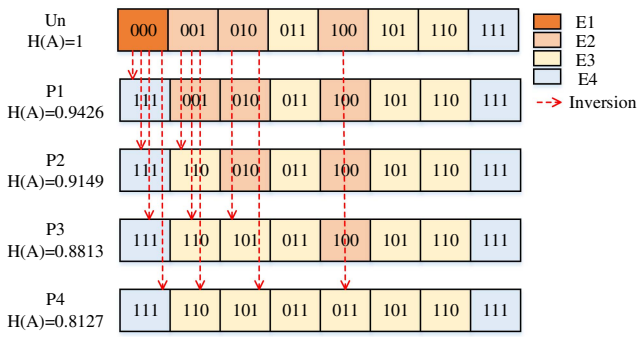

Fig. 2. Three-symbol ELA implementation process.

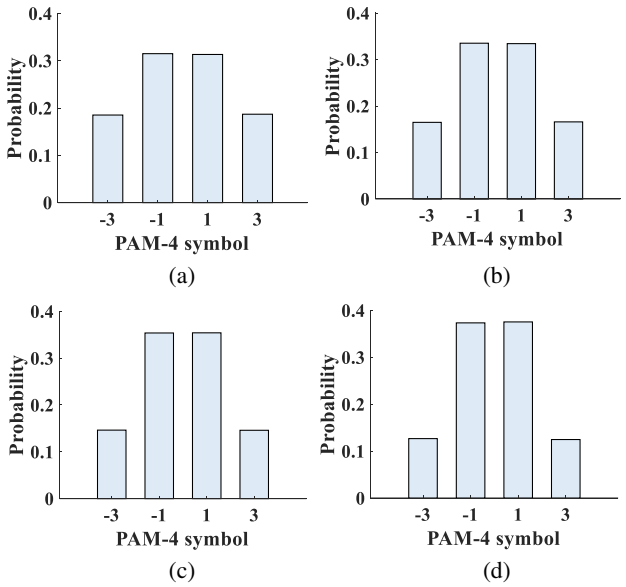

Fig. 3. Four probability distributed PAM-4 signals based on three-symbol ELA. (a) P1, (b) P2, (c) P3, and (d) P4.

signal with the P1 distribution can be yielded according to the inversion rule shown in the second row of Fig. 2, and probabilities of various energy levels are given by

$$P(E_1) = 0, \quad P(E_2) = 3/8, \quad P(E_3) = 3/8, \quad P(E_4) = 2/8. \tag{5}$$

Meanwhile, in the three-amplitude bit combinations with energy E_1 to E_4, the probabilities of "0" are 1, 2/3, 1/3, and 0, respectively. Probabilities of "0" and "1" can be calculated with encoded amplitude bits of P1 to P4 distributions according to different probabilities of various energy levels,

$$\begin{cases} P(0) = P(E_1) \times 1 + P(E_2) \times 2/3 + P(E_3) \times 1/3 + P(E_4) \times 0 \\ P(1) = 1 - P(0) \end{cases}. \tag{6}$$

According to Eqs. (5) and (6), probability distributions of "0" and "1" in P1 can be calculated. Figure 3 shows the PS-PAM-4 signals with four different probability distributions (P1 to P4) based on the three-symbol ELA method. With similar three-symbol encoding, the CAP method can only generate the PS-PAM signal with the P4 distribution. Further, the method can be extended to any n-symbol ($n > 1$) achieving more distributions with lower redundancy, and probability distributions of "0" and "1" can be expressed as

$$\begin{cases} P(0) = \sum_{i=0}^{n} P(E_{i+1}) \times (n-i)/n \\ P(1) = 1 - P(0) \end{cases}, \tag{7}$$

where $E_i > E_{i+1}$ and $P(E_{i+1}) = C_n^i / 2^n$ for uniform bit sequence.

Normalized generalized mutual information (NGMI) is used as the most robust post-forward-error-correction (FEC) bit error rate (BER) prediction[14], and the NGMI of the PS-PAM signal through an additive white Gaussian noise (AWGN) channel is given by

$$\mathrm{NGMI} = 1 - [H(X) - \mathrm{GMI}]/m, \tag{8}$$

where $m = \log_2(M)$ for the PAM-M signal, and $H(X)$ is the entropy of the PS signal. Generalized mutual information (GMI) can be estimated by

$$\mathrm{GMI} = -\sum_{x \in \chi} P_X(x) \log_2[P_X(x)] + \frac{1}{N} \sum_{k=1}^{N} \sum_{i=1}^{m} \log_2 \frac{\sum_{x \in \chi_{b_{k,i}}} q_{Y|X}(y_k|x) P_X(x)}{\sum_{x \in \chi} q_{Y|X}(y_k|x) P_X(x)}, \tag{9}$$

where χ is the symbol set, and $b_{k,i}$ is the ith bit of the kth transmitted symbol. X is the transmitted symbol, Y is the received symbol, N is the number of symbols, P_X represents the prior probability, and $q_{Y|X}$ represents the conditional probability. NGMI curves of PAM-4 signals with the abovementioned P1 to P4 distributions, uniform distribution, and the PS distribution based on the CCDM are shown in Fig. 4, where PS distributions are under the same redundancy ($R_{\mathrm{DM}} = 3/4$). Obviously, PS signals have higher NGMI under the same SNR at the expense of the achieved entropy. In addition, the NGMI curve of the P4 distribution is close to that produced by the conventional CCDM, but the ELA method has lower complexity in hardware implementation.

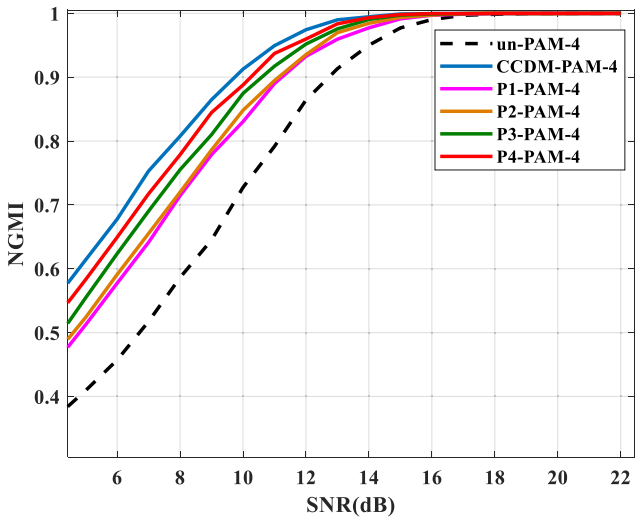

Fig. 4. NGMI curves of uniform and PS PAM-4 signals over AWGN.

3. Complexity

CCDM is a symbol-level matcher using arithmetic coding, which requires a large number of multipliers in implementation. For every 1 bit input, an interval scaling is performed. For every one-symbol output, a probability update is performed, which is in essence multiplication or division. However, ELA is a bit-level

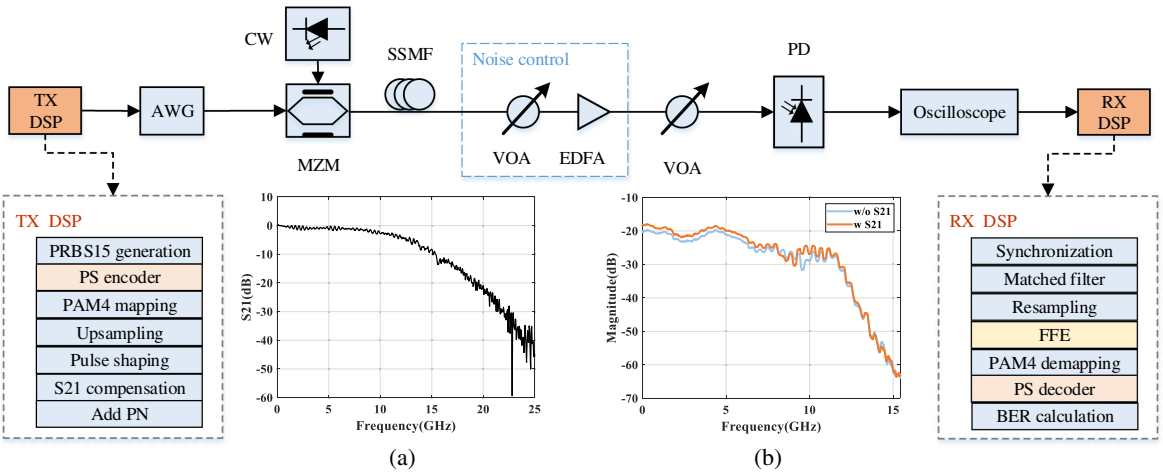

Fig. 5. Experimental setup of 25 Gbaud PAM-4 system. (a) Measured S21 parameter of the AWG; (b) measured end-to-end channel response with/without S21 compensation.

matcher by building an LUT. The complexity of the required circuitry is dominated by the number of stored bits in the LUT, and, for n-symbol encoding, $2^{nm'}(2nm'+1)$ bits are required. Complex operations such as integer addition or multiplication are not required in the coding process.

4. Experimental Setup and Results

Figure 5 shows the point to point experimental setup of 25 Gbaud IM/DD PAM-4 for intra-data-center networks. At the transmitter, pseudo-random binary sequence (PRBS) is first launched into the PS encoder, and the PS-PAM-4 data is achieved by bit-to-symbol mapping. Then, the symbol sequence is up-sampled to two samples-per-symbol (sps), and applied with a root-raised cosine (RRC) finite impulse response (FIR) filter with a roll-off factor of 0.4 for pulse shaping to mitigate the signal degradation caused by the limited bandwidth of the transmitter. The filtered and S21 compensated data is loaded into an arbitrary waveform generator (AWG), whose S21 parameter's curve is inserted, as shown by Fig. 5(a). The 3 dB bandwidth of the AWG is approximately 11 GHz. The end-to-end channel response curves with/without S21 compensation are shown in Fig. 5(b). Meanwhile, a pseudo-noise (PN) sequence is appended for signal synchronization at the receiver. After that, the electrical PAM-4 signal from the AWG is modulated into a continuous wave (CW) laser at 1550.112 nm by a single-drive Mach–Zehnder modulator (MZM). The output power of the modulated optical PAM-4 signal is about 5.7 dBm. After transmission over 2 km SSMF, a variable optical attenuator (VOA) and an erbium-doped fiber amplifier (EDFA) are used to control the noise level for BER measurement. Another VOA is used to control the optical signal power into a 10 GHz photodetector (PD). The received electrical signal is sampled by a real-time oscilloscope (RTO). The received data is first processed by the synchronization algorithm. Afterwards, the discrete digital signal passes through a matched RRC FIR filter and is re-sampled to one sps. Then, the equalization algorithm is utilized to restore the PS-PAM-4 signal. Finally, the de-mapping and PS decoding operation are implemented, and the BER is calculated.

In this work, a 25 Gbaud PAM-4 signal is transmitted over the system of approximately 10 GHz bandwidth. The received signal contains the desired signal and the pre-cursor/post-cursor ISI. Hence, we employ an FFE with a structure, as shown in Fig. 6, which consists of horizontally arranged T-delay units and tap weighting units with coefficients a_k and, thus,

$$Y(n) = \sum_{k=-M}^{M} a_k X(n+k), \tag{10}$$

where $2M+1$ ($M=15$) tap coefficients are used. Moreover, there are 32,768 symbols in the experiment and 1500 symbols for training, with the rest of them for testing. After the FFE, the training symbols are extracted to calculate the difference between the desired output and the actual output. Then, the normalized least mean square (NLMS) algorithm with lower complexity is used to adjust the tap coefficients. An iterative training process is utilized to obtain the optimum tap coefficients, and a variable step size factor accelerates the convergence.

Figure 7 shows the measured BER curves of the uniform PAM-4 signal, CCDM-PAM-4 signal, and the four PS-PAM-4 signals. The inset is the complementary cumulative distribution

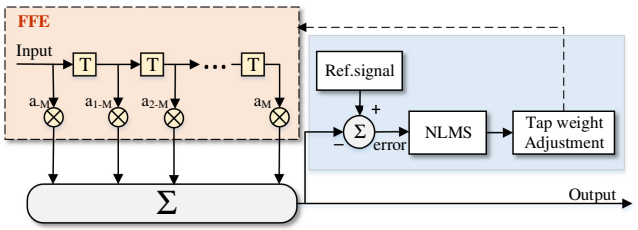

Fig. 6. Structure diagram of FFE.

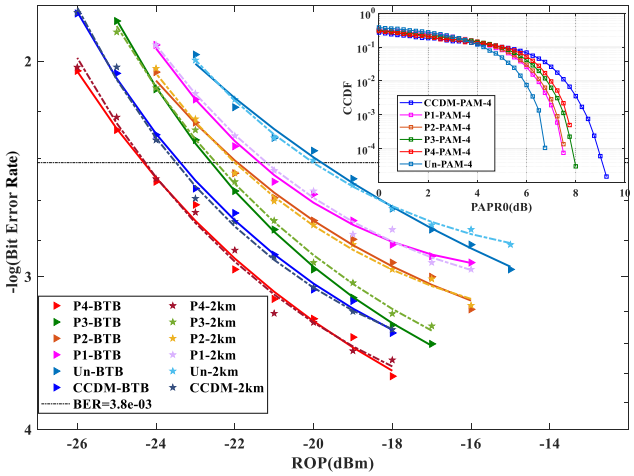

Fig. 7. Measured BER curves for 25 Gbaud uniform and PS-PAM-4 signals. The inset shows the CCDF curves for different distributions.

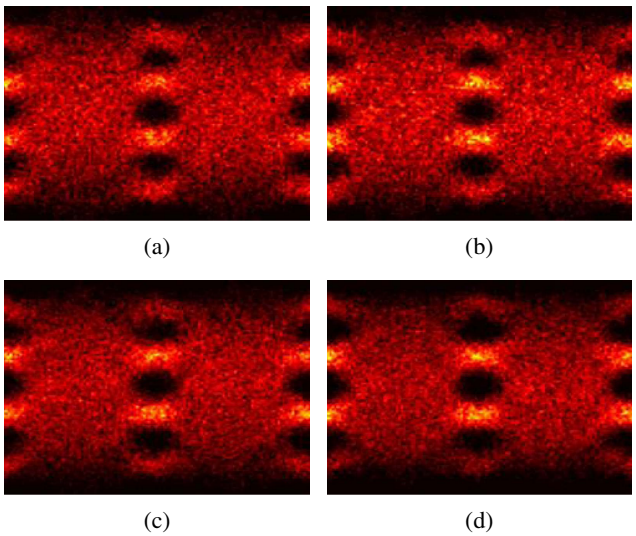

Fig. 8. Eye diagrams of PS-PAM-4 signals with various probability distributions (−20 dBm): (a) P1, (b) P2, (c) P3, and (d) P4.

function (CCDF) curve, which is mainly used to describe the peak-to-average power ratio (PAPR) of the signal. In this work, a 25 Gbaud PAM-4 signal is transmitted, and the IR of the PS signal can be expressed as in Ref. [4]:

$$\mathrm{IR} = \frac{H(A^{n_c}) + H(S^{\gamma n_c})}{n_c} = H(A) + \gamma, \tag{11}$$

where $H(A^{n_c})$ and $H(S^{\gamma n_c})$ represent the entropy of the amplitude bit and the sign bit with information for n_c symbols, respectively. For the CCDM-PAM-4 signal and P1–P4 signals, the value of γ is 1 and 2/3, respectively. The value of $H(A)$ with amplitude bits for CCDM-PAM-4 signal is 0.75. The values of $H(A)$ with other different distributions are shown in Fig. 2, so the net data rate is 50, 43.75, 40.23, 39.54, 38.70, and 36.98 Gb/s, respectively. Clearly, compared to the BTB case, the 2 km SSMF transmission induces negligible penalty, as shown by the solid and dashed curves in Fig. 7. Hence, PS-PAM-4 signals offer different trade-off choices between the receiver sensitivity and the net data rate for various application scenarios to choose the optimal distribution. Different energy-level mapping rules can be obtained by designing different LUTs, as shown in Fig. 2. As seen in the inset, the PAPR value of the signal increases with the degree of shaping. The signal generated by CCDM has the highest PAPR value, which leads to a less than ideal receiver sensitivity. Therefore, at the same baud rate and same DM rate, the performance of the signal generated by CCDM is worse than that of the P4 distribution, but better than that of the P1–P3 distributions due to its higher degree of shaping. The corresponding eye diagrams at −20 dBm are shown in Fig. 8, which show that the ISI has been mitigated by the FFE. Without the FFE, severe eye closure penalty might be induced by the ISI. By decreasing the probability of high-amplitude signals, the opening of the eye is enlarged, thereby giving a larger margin for avoiding additive noise induced errors. As shown in Fig. 8, the PS-PAM-4 system with the probability distribution of P4 exhibits the largest margin against additive noise. Consequently, the proposed ELA method can generate multi-distributed PS signals without the requirements of adjusting the symbol length of the group and using extra comparators or multipliers.

5. Conclusion

In this work, we propose an ELA DM method, which can generate multi-distributed PS-PAM-4 signals through energy-level allocation of amplitude bits. We successfully demonstrated the 2 km SSMF transmission of 25 Gbaud multi-distributed PS-PAM-4 signals in an approximately 10 GHz bandwidth system with a low-complexity linear equalization.

Acknowledgement

This work was supported by the National Natural Science Foundation of China (No. 62075147).

References

1. G. Liu, L. Zhang, T. Zuo, and Q. Zhang, "IM/DD transmission techniques for emerging 5G fronthaul, DCI, and metro applications," J. Lightwave Technol. **36**, 560 (2018).
2. A. Raza, K. Zhong, S. Ghafoor, S. Iqbal, M. Adeel, S. Habib, M. F. U. Butt, and C. Lu, "SER estimation method for 56 GBaud PAM-4 transmission system," Chin. Opt. Lett. **16**, 040604 (2018).
3. D. Zhou, D. Lu, S. Liang, L. Zhao, and W. Wang, "Transmission of 20 Gb/s PAM-4 signal over 20 km optical fiber using a directly modulated tunable DBR laser," Chin. Opt. Lett. **16**, 091401 (2018).
4. G. Böcherer, F. Steiner, and P. Schulte, "Bandwidth efficient and rate-matched low-density parity-check coded modulation," IEEE Trans. Commun. **63**, 4651 (2015).
5. T. A. Eriksson, M. Chagnon, F. Buchali, K. Schuh, S. ten Brink, and L. Schmalen, "56 Gbaud probabilistically shaped PAM8 for data center interconnects," in *European Conference on Optical Communication* (2017).

6. Z. He, T. Bo, and H. Kim, "Probabilistically shaped coded modulation for IM/DD system," Opt. Express **27**, 12126 (2019).
7. T. Wiegart, F. Da Ros, M. P. Yankov, F. Steiner, S. Gaiarin, and R. D. Wesel, "Probabilistically shaped 4-PAM for short-reach IM/DD links with a peak power constraint," J. Lightwave Technol. **39**, 400 (2021).
8. T. Yoshida, M. Karlsson, and E. Agrell, "Hierarchical distribution matching for probabilistically shaped coded modulation," J. Lightwave Technol. **37**, 1579 (2019).
9. T. V. Ramabadran, "A coding scheme for m-out-of-n codes," IEEE Trans. Commun. **38**, 1156 (1990).
10. P. Schulte and G. Böcherer, "Constant composition distribution matching," IEEE Trans. Inf. Theory **62**, 430 (2016).
11. Y. Sha, M. Gao, M. Liu, C. Zhang, W. Chen, and Y. Yan, "IM/DD probabilistically shaped 64-QAM OFDM-PON transmission assisted by selective-mapping and flexible systematic polar code," Opt. Commun. **490**, 126912 (2021).
12. F. Kschischang and S. Pasupathy, "Optimal nonuniform signaling for Gaussian channels," IEEE Trans. Inf. Theory **39**, 913 (1993).
13. J. Cho, S. Chandrasekhar, R. Dar, and P. J. Winzer, "Low-complexity shaping for enhanced nonlinearity tolerance," in *European Conference on Optical Communication* (2016).
14. J. Cho, L. Schmalen, and P. J. Winzer, "Normalized generalized mutual information as a forward error correction threshold for probabilistically shaped QAM," in *European Conference on Optical Communication* (2017).